

Cross-View-Prediction: Exploring Contrastive Feature for Hyperspectral Image Classification

Haotian Wu^a, Anyu Zhang^b and Zeyu Cao^c

^aImperial College London, Department of Electrical and Electronic Engineerin, London, UK

^bSoochow University, School of Rail Transportation, Suzhou, ,China

^cZhejiang University, College of Electrical Engineering, Hangzhou, China

ARTICLE INFO

Keywords:

self-supervised learning, autoencoder, contrastive learning, hyperspectral imagery classification

ABSTRACT

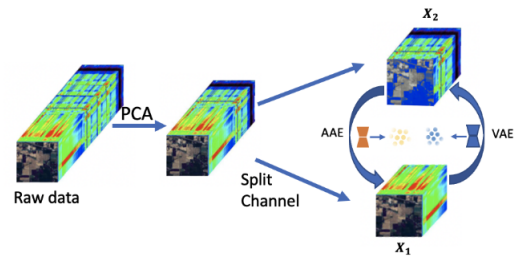
This paper presents a self-supervised feature learning method for hyperspectral image classification. Our method tries to construct two different views of the raw hyperspectral image through a cross-representation learning method. And then to learn semantically consistent representation over the created views by contrastive learning method. Specifically, four cross-channel-prediction based augmentation methods are naturally designed to utilize the high dimension characteristic of hyperspectral data for the view construction. And the better representative features are learned by maximizing mutual information and minimizing conditional entropy across different views from our contrastive network. This ‘Cross-View-Predicton’ style is straightforward and gets the state-of-the-art performance of unsupervised classification with a simple SVM classifier.

1. Introduction

Hyperspectral Image (HSI) classification problem is a fundamental task for most applications in remote sensing areas. This task has gained significant improvements from the deep learning technology for its powerful feature extraction ability. Some typical supervised feature extraction methods were developed for HSI classification, such as 1D-CNN[10], 2D-CNN[6], 3D-CNN[5], RNN[17], SSRN[29], adaptive spectral-spatial multiscale contextual feature extraction[23], FullyContNet[22]. The basic idea of these methods is to learn spatial and spectral representation features from enough data with ground truth labels. An ideal dataset is crucial to good classification performance.

But there are two main disadvantages of these supervised learning methods for the HSI classification task. Firstly, supervised methods have high requirements for datasets. Features learned by supervised methods may easily suffer from the difference between the distribution of labeled samples and the real samples. If there are not enough labels, the performance will decrease a lot. However, it is hard to provide enough HSI datasets for supervised methods, and the collection of HSI data is expensive. Secondly, supervised methods usually have poor generalization ability in HSI tasks. Models trained by the supervised techniques are generally only applicable to the current labeled HSI dataset. So researchers started to move research focus into unsupervised learning.

Ideally, unsupervised learning algorithms can address these disadvantages for the HSI by extracting representative features from the data itself without labels, which is very efficient and practical. Traditional unsupervised representation methods such as PCA[25] and ICA[21] focus on reducing the dimension of input data, which ignores the high-level information. Recent researches use deep learning methods such as auto-encoder (AE) to learn



| Our Methods | Parity Split | Sequential Split | Random Split | Overlap Split |
|-------------|--------------|------------------|--------------|---------------|
| AA(%) | 97.89 | 95.17 | 96.65 | 97.10 |
| OA(%) | 98.20 | 96.40 | 97.99 | 97.25 |

Figure 1: Our cross-view-prediction strategy applies AAE and VAE to perform the cross channel prediction tasks to construct different views of original data for contrastive learning. Table in figure shows all of these methods achieve unsupervised state-of-the-art performance in IP dataset.

the representation. AE tries to map the input data into a feature space and learn the distribution of samples. Famous AE-based methods for hyperspectral classification are SSAE[19] and 3DCAE[16], which show an impressive feature extraction ability in the remote sensing area.

Besides, contrastive learning is also a promising direction to learn the representation with high-level information. The basic rule of this method is to sample two images and learn contrastive features by minimizing the feature distance between the same image and maximizing the feature distance between different images. Contrastive learning improves the performance of downstream tasks by discriminating different samples instead of estimating the true distribution of samples. In recent researches, methods based on contrastive learning e.g. MOCO-V1[3],

ORCID(s):

MOCO-V2[9], BYOL[8] make the unsupervised performance close to fully-supervised performance in image classification tasks.

Recent research in remote sensing areas tries to combine representation learning and contrastive learning. Representation learning seems to pay more attention to each image pixel but lacks semantic-level information. Oppositely, contrastive learning pays more attention to semantic information but ignores context details. By combining representation learning and contrastive learning, methods such as ContrastNet[2], Transformer based contrastive learning[11], Spatial-Spectral Clustering methods[12] show a remarkably potential of reducing dependency on datasets and achieving state-of-the-art performance. However, their feature's representative ability still could be improved.

Different from previous methods, we propose a self-supervised hyperspectral feature learning method based on cross representation learning and contrastive learning. The whole algorithm is a cross-view-prediction style (Figure 1). Inspired by Split-AE[28], and considering the characteristic of hyperspectral images, we propose a cross-representation learning method to induce contrastive features. To be specific, hyperspectral images share redundant spectral-spatial features and preserves high-level semantics across the channel, which naturally leads to cross channel prediction tasks. To exploit the consistency of semantic information between channels, we split the input data into two subsets and force networks to predict one sub-set of the data from the another. The resulting latent codes can be seen as different views of original data and can induce better features by contrastive learning methods. We try to explore consistently semantic features by this cross-view-prediction style. Besides, this style makes feature transfer well between different sub-spaces, which explores a better representation for other unseen downstream tasks.

One novelty here is using cross-channel-prediction tasks as augmentation methods to construct different descriptions of original data, encouraging exploring contrastive features. Another novelty is treating cross-representation latent codes as different views and using a contrastive learning method to generate a better representation feature. The main idea of our contrastive learning method is to maximize the mutual information and minimize conditional entropy between two views. The pipeline is interpretable and straightforward without a requirement for negative samples.

Benefiting from our cross-view-prediction and contrastive learning strategy, we extract better features for HSI classification tasks and get a state-of-the-art performance by simply connecting a Support Vector Machine (SVM)[18]. To summarize, our contribution can be listed below:

- We propose a cross representation learning method exploring high dimension HSI data. Learning from cross-channel prediction tasks, the model implicitly

learns contrastive latent codes as augmentations in hyperspectral space.

- We propose an interpretable and straightforward self-supervised contrastive feature learning method for the HSI classification task. Specifically, our pipeline treats the cross-representation latent codes as different views of original data and optimizes the features from information theory. We achieved state-of-the-art hyperspectral imagery classification performance only with the help of a weak classifier SVM in several standard datasets.

2. Related work

2.1. Autoencoder based feature learning

Autoencoder (AE) is commonly used in unsupervised learning and representation learning structure. Traditional autoencoder has no constraints over latent space. VAE and AAE is then proposed to optimize the distribution of the latent code, which makes latent code more representative and disentangled. Variational autoencoder(VAE)[13] uses Kullback–Leibler (KL) divergence and reparameterization method to set latent code into norm distribution. Also, a reconstruction phase ensures the distribution of generated image and input image to be close. Adversary autoencoder (AAE)[15] uses a generative adversarial network (GAN) style to set adversary restriction over latent code. The encoder of AAE plays the role of a generator to generate the latent code into target distribution and fool discriminator. The discriminator is trained to distinguish the randomly sampled norm distribution and latent code. Besides, a reconstruction phase also ensures the distribution of generated image and input image to be close. Some past research[2][24][27] on representation learning for hyperspectral images shows the latent codes generated by VAE and AAE are relatively fixed and better representative. So VAE and AAE are widely used in hyperspectral tasks for better classification performance.

2.2. Unsupervised feature learning

ContrastNet[2] treats different encoders as augmentation functions, and uses the discriminative learning method (prototypical contrastive learning) to fuse different feature spaces. This method shows the potential of getting more representative features by applying contrastive learning over different feature spaces. Different from ContrastNet, we apply a cross representation learning strategy to induce a contrastive feature and treat cross representations as different 'views' of original data to optimize. Besides, compared with the complex M-N steps optimizing process, our pipeline has no requirements for negative data, which is more straightforward.

Split-brain-autoencoder (Split-AE)[28] is a typical cross-channel prediction unsupervised pipeline. Split-AE trains two disjoint sub-networks to predict one subset of raw data from another subset of raw data. Training these cross-channel encoders to predict 'unseen' channels makes Split-AE implicitly learn contrastive features for other

Algorithm 1 Cross-View-prediction Algorithm

Stage 1: Cross representation learning

1: $\mathcal{Z}_{vae}, \mathcal{Z}_{aae} = \mathcal{H}(X_{raw})$ \triangleright learn cross-representation

Stage 2: Contrastive learning

1: $\mathcal{Z}_{con} = \mathcal{P}(\mathcal{Z}_{vae}, \mathcal{Z}_{aae})$ \triangleright learn contrastive features

tasks. Inspired by Split-AE[28], a cross representation learning strategy is naturally designed for the hyperspectral image because of its high channel dimension. In this way, we explore contrastive features and construct different descriptions of the raw data for the later contrastive learning stage.

Bootstrap Your Own Latent (BYOL)[8] is a self-supervised method without the requirement of negative data. It uses one online and one target network with the same structure to learn from each other and applies a moving average update strategy. Some other self-supervised methods, such as SimSiam [4] and PixContrast[26], also use similar ideas. Inspired by this, we use this style to optimize our contrastive multi-descriptions task. Because of the exponential moving average strategy and information entropy-based loss, our method can avoid trivial solutions. Also, removing the need for negative samples makes the pipeline efficient and straightforward.

3. Proposed Method

Our cross-view-prediction style can be divided into two-stage: cross representation learning stage and contrastive learning stage (Algorithm 1). $\mathcal{Z}_{aae}, \mathcal{Z}_{vae}, \mathcal{Z}_{con}$ are features extracted by AAE, VAE and contrastive net. \mathcal{H} and \mathcal{P} represent cross-representation and contrastive learning process. In the first stage, we trained VAE and AAE to learn a pair of representations of original data from cross-channel-prediction tasks. In the second stage, we use a contrastive network to optimize representation features.

3.1. Cross representation learning

One typical characteristic of our method is using a cross-representation learning style. We try to explore the contrastive features from hyperspectral data itself. Considering the consistency of semantic information between adjacent channels, we split the input data into two subsets along the channel direction and force networks to predict one subset of the data from the another. Ideally, there is no consistent information loss in this cross prediction task from the original data[28].

We propose four cross representation learning methods for hyperspectral self-supervised learning tasks to get different views that preserve consistent information. They are parity split, sequential split, random split, overlapping split. Intuitively, we see these learning methods as augmentation methods and treat resulting latent codes as different views with consistent semantics. The pipeline of these four augmentation methods is shown in Figure 1 and

Algorithm 2 Cross representation learning for HSI

Input:

Raw hypersepctral image: X_{raw}

VAE encoder, AAE encoder: $\mathcal{F}_{\eta E}, \mathcal{F}_{\mu E}$

```

1: for each batch do
2:    $X = PCA(X_{raw})$ 
3:    $X \in \mathbb{R}^{H \times W \times C}$   $\triangleright$  apply PCA into original data
4:   if ‘Parity split’ then
5:      $X_1 = X[:, :, 0 : C : 2], X_2 = X[:, :, 1 : C : 2]$ 
6:   else if ‘Sequential split’ then
7:      $X_1 = X[:, :, 0 : \frac{C}{2}], X_2 = X[:, :, \frac{C}{2} : C]$ 
8:   else if ‘Random split’ then
9:      $X_{rs} = \mathcal{RS}_{\frac{C}{6}}(\frac{C}{2} : C), X_2 = X[:, :, \frac{C}{3} : C]$ 
10:     $X_1 = Cat(X[:, :, 0 : \frac{C}{2}], X_{rs})$ 
11:   else if ‘Overlapping split’ then
12:     $X_1 = X[:, :, 0 : \frac{2}{3}C], X_2 = X[:, :, \frac{1}{3}C : C]$ 
13:     $\mathcal{Z}_{vae} = \mathcal{F}_{\eta E}(X_1)$   $\triangleright$  Train VAE representation
14:     $\mathcal{Z}_{aae} = \mathcal{F}_{\mu E}(X_2)$   $\triangleright$  Train AAE representation
Output: VAE and AAE representation view:  $\mathcal{Z}_{vae}, \mathcal{Z}_{aae}$ 
    
```

Algorithm 2. $X[:, :, :, 0 : C : 2]$ means taking channels with index from 0 to C with step 2. $:$ means no operation along this dimension.

We trained AAE and VAE separately because their latent codes are similar but slightly different, and these two structures work best in remote sensing areas[2]. For the raw hypersepctral image $X_{raw} \in \mathbb{R}^{H \times W \times C_h}$, we apply the Principal component analysis (PCA) algorithm[25] as pre-process, getting the data $X \in \mathbb{R}^{H \times W \times C}$. We then apply our augmentation methods to split the data X into two parts $X_1 \in \mathbb{R}^{H \times W \times C_1}, X_2 \in \mathbb{R}^{H \times W \times C_2}$. H, W are patch size we created for our dataset. To retain all information from original data, X_1 and X_2 should loop through all data $X \subseteq (X_1 \cup X_2)$.

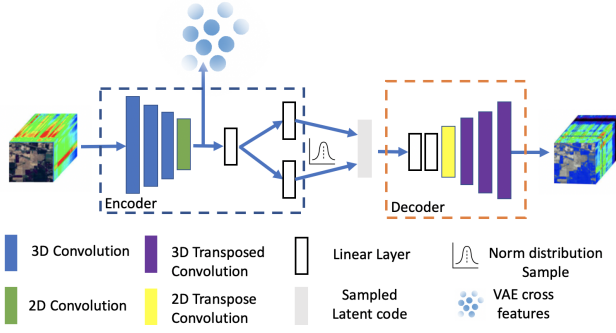
For ‘Parity split’: We use odd channels subset as X_1 , even channels subset as X_2 . X_1 and X_2 are designed as adjacent channel styles to exploit robust consistency.

For ‘Sequential split’: We use the first-half channels as X_1 and the left as X_2 . X_1 and X_2 are designed as one after the other style to exploit more long-term consistency.

For ‘Random split’: X_1 is stacked by a fix $\frac{C}{2}$ channels part and $\frac{C}{6}$ random channels part along channel dimension. X_2 is fixed when working as prediction ground truth. $\mathcal{RS}_{\frac{C}{6}}(\frac{C}{2} : C)$ means random sampling $\frac{C}{6}$ channels from index $\frac{C}{2}$ to index C . Cat means concatenation operation along channel dimension. By introducing extra random information, we want to make the strategy explore extra more information on its consistency.

For ‘Overlap split’: We use first $\frac{2}{3}$ channels as X_1 , second $\frac{2}{3}$ channels as X_2 . X_1 and X_2 are designed overlapping to encourage trade-off between long term and short term consistency.

After split augmentation, we got two views X_1 and X_2


Figure 2: VAE structure for hyperspectral image

for VAE and AAE. We trained a VAE model \mathcal{F}_1 with data X_1 to predict X_2 , $\hat{X}_2 = \mathcal{F}_1(X_1)$. Symmetrically, we use same strategy to train a AAE model \mathcal{F}_2 with data X_2 to predict X_1 , $\hat{X}_1 = \mathcal{F}_2(X_2)$. The losses used in this training process can be mean squared error loss (Equation 1) or standard cross-entropy. W, H, C is the size of the images X, Y .

$$\mathcal{L}_{mse}(X, Y) = \frac{1}{W * H * C} \sum_{h,w,c} \|X - Y\|^2 \quad (1)$$

For fair comparison without label introduced, we use mean square loss $\mathcal{L}_{mse}(\mathcal{F}_1(X_1), X_2)$, and $\mathcal{L}_{mse}(X_1, \mathcal{F}_2(X_2))$ in our VAE and AAE training.

3.1.1. VAE module

To perform this cross channel prediction task $\hat{X}_2 = \mathcal{F}_1(X_1)$, we designed a VAE feature extractor. The structure of this extractor is shown in Figure 2.

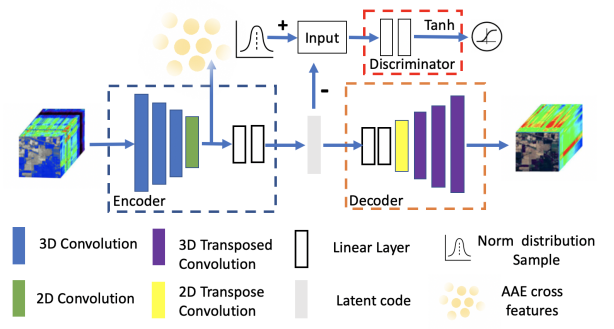
In Encoder, we used 3D and 2D CNN to generate latent code, learning more channel information with low computation complexity. Similar to the original VAE[13], two FC layers mapped features into mean μ and variance σ . We generated latent code by reparametering a norm distribution (Equation 2), where X is sampled from a norm distribution.

$$z = \mu + \sigma \times X, X \sim N(0, 1) \quad (2)$$

In Decoder, symmetrical to Encoder, several FC layers, 2D and 3D transposed CNNs are used to recover the inputs. Loss function of VAE is Equation 3.

$$\begin{aligned} \mathcal{L}_{vae} &= \mathcal{L}_{mse}^{vae} + L_{kl} \\ \mathcal{L}_{mse}^{vae} &= \mathcal{L}_{mse}(\mathcal{F}_1(X_1), X_2) \\ \mathcal{L}_{kl} &= \frac{1}{2} \sum_i^N (\mu_i^2 + \sigma_i^2 - \log \sigma_i^2 - 1) \end{aligned} \quad (3)$$

\mathcal{L}_{mse}^{vae} is mean square error loss, ensuring the reconstruction performance. $\mathcal{F}(X_1)$. L_{kl} is distribution loss, minimizing the KL divergence between latent code and normal distribution.


Figure 3: AAE structure for hyperspectral image

3.1.2. AAE module

Intuitively, we want to design two feature extractors in the Siamese style. So we also design an AAE module siamese to VAE to perform the prediction $\hat{X}_1 = \mathcal{F}_2(X_2)$. The structure of this feature extractor is shown in Figure 3.

The encoder and decoder have the same structure as the previous VAE. The different part is encoder here also plays a role of GAN generator. Similar to the original AAE[15], we feed the latent code and a random norm distribution sample into a discriminator. There are two-phase in AAE training: the reconstruction phase and the regularization phase. In reconstruction phase, we train the encoder and decoder with loss \mathcal{L}_{mse}^{aae} in Equation 4.

$$\mathcal{L}_{mse}^{aae} = \mathcal{L}_{mse}(\mathcal{F}_2(X_2), X_1) \quad (4)$$

In the regularization phase, we optimize the discriminator first and then the generator. For the loss, we use the Wasserstein GAN (WGAN)[1] loss. \mathcal{L}_G is generator loss.

$$\mathcal{L}_G = E_{x \sim P_g} [D(x)] - E_{x \sim P_r} [D(x)] \quad (5)$$

$$\mathcal{L}_D = -E_{x \sim P_g} [D(x)] \quad (6)$$

\mathcal{L}_D is discriminator loss. $D(x)$ means the output of the discriminator with input x . $x \sim P_g$ means sampling input from distribution P_g . P_r is the distribution of real samples. P_g is the distribution of fake samples.

3.2. Contrastive learning

Another typical characteristic of our method is that we treat mutual prediction features as different views of the original data and design a contrastive learning method to optimize the features further.

Figure 4 is an overview of our contrastive learning method. We feed the VAE representation view and AAE representation view into the pipeline (both are treated as online net once and target network once symmetrically). Our method consists of Contrastive Encoder module (f_θ, f_ξ), Projection module (p_θ, p_ξ) and Prediction module

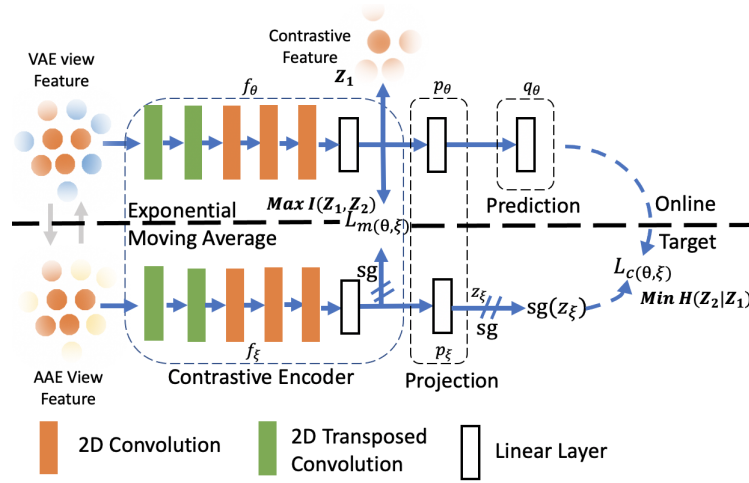


Figure 4: Structure of the system, sg means stop-gradient, $I(Z_1, Z_2)$ means mutual information between latent Z_1 and Z_2 , $H(Z_2|Z_1)$ means conditional entropy

q_θ , which all share the same structure for online and target nets.

Because our cross representation naturally learned some good contrastive features, our Contrastive Encoder module is simple with several 2D CNN and 2D Transpose CNN. The projection and prediction module consists of several FC layers, which is similar to BYOL[8], SimSiam[4].

The detailed algorithm is shown in Algorithm 3. We use Contrastive Encoder module to encode input features and induce a more representative contrastive feature. We use two information entropy strategies to promote this purpose: maximizing mutual information and minimizing the conditional entropy between input features, which is simple and interpretable.

Algorithm 3 Contrastive learning for HSI

Input:

VAE and AAE representation view: $\mathcal{F}_{vae}, \mathcal{F}_{aae}$

Online encoder, projector, predictor: $f_\theta, p_\theta, q_\theta$

Target encoder, projector, Optimizer: f_ξ, p_ξ, Opt

```

1: for each batch do
2:    $\mathcal{F}_{vae}, \mathcal{F}_{aae}$       ▷ Sample a pair of features
3:    $f_1 = f_\theta(\mathcal{F}_{vae}), f_2 = f_\theta(\mathcal{F}_{aae})$   ▷ Online feature
4:    $f'_1 = f_\xi(\mathcal{F}_{vae}), f'_2 = f_\xi(\mathcal{F}_{aae})$   ▷ Target feature
5:    $\mathcal{L}_m(Z_1, Z_2) = -(I(Z_1, Z_2) + \alpha(H(Z_1) + H(Z_2)))$ 
6:                                     ▷ Mutual Loss
7:    $z_1 = p_\theta(f_1), z_2 = p_\theta(f_2)$       ▷ Online projection
8:    $z'_1 = p_\xi(f'_1), z'_2 = p_\xi(f'_2)$     ▷ Target projection
9:    $\mathcal{L}_c = -2(\frac{\langle q_\theta(z_1), z'_1 \rangle}{\|q_\theta(z_1)\| \|z'_1\|} + \frac{\langle q_\theta(z_2), z'_2 \rangle}{\|q_\theta(z_2)\| \|z'_2\|})$ 
10:                                     ▷ Conditional loss
11:    $\mathcal{L} = \lambda \mathcal{L}_m + \mathcal{L}_c$               ▷ Loss function
12:    $\theta \leftarrow Opt(\theta, \nabla_\theta \mathcal{L})$       ▷ Update online network
13:    $\xi \leftarrow \tau \xi + (1 - \tau) \theta$      ▷ Update target network

```

Output: Online encoder: f_θ

3.2.1. Maximize mutual information

Instead of maximizing the lower bound of mutual information, we use a mutual-information-based loss (Equation 7) to optimize the mutual information directly. $I(Z_1, Z_2)$ means mutual information between Z_1, Z_2 . H is the information entropy. α is a regularization parameter. With this loss \mathcal{L}_m , we maximize mutual information between Z_1 and Z_2 . Also, we try to maximize the information entropy of Z_1 and Z_2 to preserve more information for each view, which avoids trivial solutions.

$$\mathcal{L}_m(Z_1, Z_2) = -(I(Z_1, Z_2) + \alpha(H(Z_1) + H(Z_2))) \quad (7)$$

To compute the $I(Z_1, Z_2)$ and $H(Z_i)$, we define the joint probability distribution $P(z_1, z_2) \in (d, d)$ in Equation 8.

$$P(z_1, z_2) = S(Z_1)S(Z_2)^T \quad (8)$$

$P(z_1, z_2)$ shows the correlation between two random variables of representations. S is Softmax operation. And then we could compute the Equation 7 by Equation 9.

$$\mathcal{L}_m = - \sum_{i=1}^d \sum_{j=1}^d P(i, j) \ln \frac{P(i, j)}{P_i^{\alpha+1} P_j^{\alpha+1}} \quad (9)$$

d is the dimension of the our representation feature. α is a normalization parameter for the loss.

3.2.2. Minimize conditional entropy

Our network uses a prediction operation after the Projection module to minimize the conditional entropy, which encourages maximizing the overlapping information over different views. As we know, when two views are fully overlapped, then $H(Z_2|Z_1) = 0$, which means the resulting feature is most representative. This design can encourage contrastive encoder to encode more representative information[8][4].

To reduce conditional entropy, common methods is to introduce a variational Gaussian distribution[7]. In practice, this minimization problem can also be converted into Equation 10[14], where G^i means a mapping between views. Our network (Figure 4) and loss \mathcal{L}_c (Equation 11) is designed based on this, where we compute the distance between the prediction output $q_\theta(z_i)$ and z'_i with l2-normalization.

$$\min \|Z_1 - G^1(Z_2)\|^2 + \|Z_2 - G^2(Z_1)\|^2 \quad (10)$$

$$\mathcal{L}_c = 2 - 2\left(\frac{\langle q_\theta(z_1), z'_1 \rangle}{\|q_\theta(z_1)\| \|z'_1\|} + \frac{\langle q_\theta(z_2), z'_2 \rangle}{\|q_\theta(z_2)\| \|z'_2\|}\right) \quad (11)$$

z_1 and z'_1 are extracted contrastive features from VAE and AAE views, the same as the z_2 and z'_2 . q_θ is a prediction operation.

3.2.3. Update strategy

We symmetrize the training process by exchanging VAE cross-feature and AAE cross-feature into online and target net. We use the weighted loss (Equation 12) to optimize the online net by backpropagation and use the exponential moving average strategy to update the target net (Equation 13,14).

$$\mathcal{L} = \lambda \mathcal{L}_m + \mathcal{L}_c \quad (12)$$

$$\theta \leftarrow Opt(\theta, \nabla_\theta L) \quad (13)$$

$$\xi \leftarrow \tau \xi + (1 - \tau)\theta \quad (14)$$

λ is the loss weight. $\mathcal{L}_m, \mathcal{L}_c$ can be computed by Equation (9, 11). τ is a target delay rate. This updating strategy can avoid some trivial solutions. Opt is the optimizer.

4. Experiments and analysis

We use a simple classifier SVM to achieve the state-of-the-art classification performance to show the representation ability of our extracted features.

4.1. Datasets

We apply our method to three standard datasets for the hyperspectral classification task: Indian Pines(IP) dataset, University of Pavia(PU) dataset, and Salinas Scene(SA) dataset.

IP dataset consists of 145×145 pixels with 220 spectral reflectance bands in the wavelength range $0.4 - 2.5 \times 10^{-6}m$. There are 16 classes of ground truth. Without the bands covering water absorption, 200 bands were considered in the experiments. The main challenge in this dataset is an unbalanced number of labels. Some class

Table 1
Details of IP dataset

| IP dataset | | |
|---------------------------|-------|---------------|
| Class | Index | Sample number |
| Alfalfa | 0 | 46 |
| Corn-notill | 1 | 1428 |
| Corn-mintill | 2 | 830 |
| Corn | 3 | 237 |
| Grass-pasture | 4 | 483 |
| Grass-trees | 5 | 730 |
| Grass-pasture-mowed | 6 | 28 |
| Hay-windrowed | 7 | 478 |
| Oats | 8 | 20 |
| Soybean-notill | 9 | 972 |
| Soybean-mintill | 10 | 2455 |
| Soybean-clean | 11 | 593 |
| Wheat | 12 | 205 |
| Woods | 13 | 1265 |
| Building-Grass-Tree-Drive | 14 | 386 |
| Stone-Steel-Towers | 15 | 93 |
| Total | | 10249 |

Table 2
Details of PU ataset

| PU dataset | | |
|----------------------|-------|---------------|
| Class | Index | Sample number |
| Asphalt | 0 | 6631 |
| Meadows | 1 | 18649 |
| Gravel | 2 | 2099 |
| Trees | 3 | 3064 |
| Painted metal sheets | 4 | 1345 |
| Bare Soil | 5 | 5029 |
| Bitumen | 6 | 1330 |
| Self-Blocking-Bricks | 7 | 3682 |
| Shadows | 8 | 947 |
| Total | | 42776 |

Table 3
Details of PU ataset

likes Soybean-mintill has 2455 samples, but class like Oats only has 20 samples. The detail can be seen in the table 1 below.

IP dataset (16 classes in ground truth) consists of 145×145 pixels with 220 spectral reflectance bands. The main challenge in the IP dataset is the unbalanced number of labels.

Indian Pines (IP) dataset:

PU dataset (9 classes) consists of 610×340 pixels with 103 spectral reflectance bands. The main challenges in PU dataset are its complex background and many discontinuous pixels.

University of Pavia(PU) dataset:

PU dataset consists of 610×340 pixels with 103 spectral reflectance bands in the wavelength range $0.43 - 0.86 \times 10^{-6}m$. There are nine classes in the ground truth. The main challenges in this dataset are its complex background and many discontinuous pixels. The detail can be seen in the table 2 below.



Figure 5: t-SNE visualization of contrastive features in the IP dataset.

| SA dataset | | |
|---------------------------|-------|---------------|
| Class | Index | Sample number |
| Brocoli-green-weeds1 | 0 | 2009 |
| Brocoli-green-weeds2 | 1 | 3726 |
| Fallow | 2 | 1976 |
| Fallow-rough-plow | 3 | 1394 |
| Fallow-smooth | 4 | 2678 |
| Stubble | 5 | 3959 |
| Celery | 6 | 3579 |
| Grapes-untrained | 7 | 11271 |
| Soil-vinyard-develop | 8 | 6203 |
| Corn-senesced-green-weeds | 9 | 3278 |
| Lettuce-romaine-4wk | 10 | 1068 |
| Lettuce-romaine-5wk | 11 | 1927 |
| Lettuce-romaine-6wk | 12 | 916 |
| Lettuce-romaine-7wk | 13 | 1070 |
| Vinyard-untrained | 14 | 7268 |
| Vinyard-vertical-trellis | 15 | 1807 |
| Total | | 54129 |

Table 4
Details of SA dataset

SA dataset (16 classes) consists of 512×217 pixels with 224 spectral reflectance bands. This dataset is simple compared with the IP dataset and PU dataset.

Salinas Scene(SA) dataset:

SA dataset consists of 512×217 pixels with 224 spectral reflectance bands in the wavelength range $0.36 - 2.5 \times 10^{-6}m$. Ignoring the bands covering water absorption, 204 bands remain in the experiments. There are 16 classes in the ground truth. This dataset is simple compared with the IP dataset and PU dataset. The detail can be seen in the table 4 below.

4.2. Model implementation

To train SVM, we use 5% samples in each class for training, and the left is used for testing in SA dataset (because the dataset is simple). However, in IP and PU

datasets, 10% samples are used for training; the left is used for testing.

The shape of patches after PCA is (27, 27, 30). We do experiments on all four augmentation methods. Latent codes from VAE and AAE are 128 dimension vectors.

For AAE and VAE, Adam optimizers with a learning rate: 0.001 and weight decay: 0.0005. Two SGD optimizers for AAE has learning rate: 0.0001 (generator) and learning rate: 0.00005 (discriminator). The batch size is 256. We train the AAE module for 30 epochs and VAE for 40 epochs for the best performance.

For contrastive learning, we use an Adam optimizer with a learning rate of $3e - 4$, weight decay is set to 0.001. We train 200 epochs and select the best feature. To normalize loss, $\alpha = 9$, $\lambda = 100$. Results are evaluated by average accuracy (AA) and overall accuracy (OA) (Equation 15).

$$\begin{aligned}
 OA(\%) &= \frac{N_p}{N_a} \\
 AA(\%) &= \frac{1}{N} \sum_{i=1}^N c_i
 \end{aligned} \tag{15}$$

N is class number, c_i is each class classification accuracy. N_p is the number of accurate classification samples. N_a is the total number of all samples.

4.3. Experiments Results

4.3.1. Cross representation experiments

As PU and SA datasets are simple, all our strategies work very well. We compare our different augmentation methods in the IP dataset. Table in Figure 1 shows HSI classification performance of our cross-view-prediction strategies. All four cross-prediction strategies have good performance, showing that our cross-view-prediction style encourages the consistency of semantic information and suits HSI tasks.

The ‘Parity Split’ strategy works best, which is used to compare with other algorithms later. Random Split and Overlap Split also work state-of-the-art, which shows the

| Class | Supervised Feature Extraction | | | | Unsupervised Feature Extraction | | | |
|-------|-------------------------------|--------|-------|--------------|---------------------------------|---------------|--------------|---------------|
| | SLGDA | 1D-CNN | S-CNN | 3DCAE | AAE | VAE | ContrastNet | Ours model |
| 0 | 39.62 | 43.33 | 83.33 | 90.48 | 100.00 | 100.00 | 85.37 | 92.35 |
| 1 | 85.56 | 73.13 | 81.41 | 92.49 | 81.63 | 78.78 | 97.15 | 96.95 |
| 2 | 74.82 | 65.52 | 74.02 | 90.37 | 95.27 | 92.37 | 97.95 | 97.86 |
| 3 | 49.32 | 51.31 | 71.49 | 86.90 | 99.22 | 97.34 | 95.62 | 93.64 |
| 4 | 95.35 | 87.70 | 90.11 | 94.25 | 95.17 | 96.09 | 94.82 | 98.40 |
| 5 | 95.59 | 95.10 | 94.06 | 97.07 | 98.73 | 98.27 | 96.80 | 99.40 |
| 6 | 36.92 | 56.92 | 84.61 | 91.26 | 96.00 | 98.67 | 70.67 | 100.00 |
| 7 | 99.75 | 96.64 | 98.37 | 97.79 | 99.84 | 99.77 | 98.68 | 99.07 |
| 8 | 5.00 | 28.89 | 33.33 | 75.91 | 96.30 | 98.15 | 70.37 | 100.00 |
| 9 | 69.11 | 75.12 | 86.05 | 87.34 | 87.01 | 78.86 | 97.45 | 97.71 |
| 10 | 89.91 | 83.49 | 82.98 | 90.24 | 89.08 | 81.75 | 98.40 | 98.73 |
| 11 | 86.78 | 67.55 | 73.40 | 95.76 | 93.51 | 90.64 | 93.57 | 94.19 |
| 12 | 99.51 | 96.86 | 87.02 | 97.49 | 98.56 | 98.56 | 95.32 | 98.92 |
| 13 | 96.45 | 96.51 | 94.38 | 96.03 | 95.73 | 93.24 | 98.51 | 99.91 |
| 14 | 61.79 | 39.08 | 75.57 | 90.48 | 97.31 | 97.02 | 96.73 | 99.14 |
| 15 | 84.16 | 89.40 | 79.76 | 98.82 | 98.02 | 98.81 | 79.76 | 100.00 |
| AA(%) | 73.10 | 71.66 | 84.44 | 92.04 | 95.09 | 93.51 | 91.78 | 97.89 |
| OA(%) | 85.19 | 79.66 | 80.72 | 92.35 | 91.80 | 88.03 | 97.08 | 98.20 |

Table 5
Evaluation in Indian Pines dataset

| Class | Supervised Feature Extraction | | | | Unsupervised Feature Extraction | | | |
|-------|-------------------------------|--------|-------|-------|---------------------------------|-------|-------------|--------------|
| | SLGDA | 1D-CNN | S-CNN | 3DCAE | AAE | VAE | ContrastNet | Ours model |
| AA(%) | 96.01 | 94.73 | 97.39 | 97.45 | 98.73 | 97.67 | 99.48 | 99.70 |
| OA(%) | 93.31 | 91.30 | 97.92 | 95.81 | 97.10 | 95.23 | 99.60 | 99.82 |

Table 6
Evaluation in Salinas dataset

advantage of our cross prediction style in finding robust and consistent information from random sampling. Sequential Split works a bit worse. It may be because our simple network has a limited ability to extract long-term consistency when faced with this simple split strategy.

Figure 5 shows the t-SNE visualization[20] of the extracted features. Each color means one class. In our style, we could see AAE and VAE learned compact and discriminative features. It is hard to discriminate which distribution is better, but our contrastive learning method tries to fuse VAE and AAE feature distribution, which tends to make features more compact and informative.

4.3.2. Contrastive learning experiments

Table 5, Table 6 and Table 7 show HSI classification experiments for IP, SA and PU dataset separately. Results in bold are the best performance. Some best performance are quoted from[16][2]. Our model gets state-of-the-art performance with the highest OA and AA in all of three datasets.

For the IP dataset, supervised feature learning methods have worse performance, which may result from the unbalanced dataset. However, our method doesn't work best in all classes. Contrastive learning method sometimes may confuse the feature representation for overlapping classes.

For the PU dataset, unsupervised feature learning methods outperform other supervised methods. We think it

is because of its complex background, leading to trivial over-fitting results for supervised methods.

For the SA dataset, a simple dataset, our method gains 100% results in most classes and still achieves the best accuracy. It shows our method indeed further extracts more information than the other unsupervised learning methods.

In summarization, unsupervised feature learning methods are better solutions for HSI classification tasks, whose labelled datasets are usually imbalanced and rare. Among unsupervised algorithms, our method gains the best performance and outperforms all other existing methods. This impressive result shows features from our cross-view-prediction style have a better representation ability. Also, results show our contrastive learning strategy further enhances the performance and optimizes the trade-off between the AAE feature view and the VAE feature view.

5. Extra ablation experiments

We have seen that our cross-view-prediction style has good performance in extracting HSI contrastive features. Cross-prediction and contrastive learning are two main strategies in our methods. In this section, we do the ablation experiments to check the effectiveness of these two methods.

| Class | Supervised Feature Extraction | | | | Unsupervised Feature Extraction | | | |
|-------|-------------------------------|--------|-------|-------|---------------------------------|-------|-------------|--------------|
| | SLGDA | 1D-CNN | S-CNN | 3DCAE | AAE | VAE | ContrastNet | Ours model |
| AA(%) | 91.86 | 87.34 | 94.75 | 95.36 | 98.03 | 94.16 | 98.83 | 99.30 |
| OA(%) | 94.15 | 89.99 | 92.78 | 95.39 | 98.14 | 94.53 | 99.46 | 99.78 |

Table 7
Evaluation in University of Pavia dataset



Figure 6: t-SNE visualization of features in the IP dataset.

Table 8
Ablation experiments of cross-prediction style

| | VAE | Cross-VAE | AAE | Cross-AAE |
|-------|-------|--------------|-------|--------------|
| AA(%) | 88.65 | 93.85 | 93.28 | 95.71 |
| OA(%) | 82.02 | 91.33 | 90.46 | 92.13 |

Data in bold are the best performance.

Table 9
Ablation experiments of contrastive learning

| | Cross-VAE | Cross-AAE | Contrastive |
|-------|-----------|-----------|--------------|
| AA(%) | 93.85 | 95.71 | 97.89 |
| OA(%) | 91.33 | 92.13 | 98.20 |

Data in bold are the best performance.

5.1. Cross representation ablation experiments

One of the purposes of our cross-prediction design is to construct a pair of views for our contrastive learning process. Another purpose is to learn a contrastive feature implicitly.

Here we do the ablation experiments for this cross representation learning method to validate the effects of our cross-prediction design. We expect it could bring extra benefits of better contrastive features. We directly apply an SVM over the contrastive features from our cross-prediction tasks and standard autoencoders. We use the same channel numbers (15 channels) to predict features in the standard representation learning for a fair comparison, which uses less information from the implementation in ContrastNet. We used the IP dataset (10% data used in the training process) to show classification performance.

Table 8 shows classification experiment results from cross-representation features and standard autoencoders features. It shows our contrastive features also have better performance than standard features. It means, when making features a transferable pair for contrastive learning tasks, the cross-representation style also improves the performance. For VAE, it has a significant improvement. For AAE, both methods work well.

We also visualize the features from the standard

autoencoder and our cross-prediction method by t-SNE method. From Figure 6, we can see features from our method are more compact. For VAE, some classes of our cross-VAE features are more discriminative, which shows the advantage of our methods in the VAE pipeline. For AAE, both work well. Features from our methods are more compact and discriminative too.

5.2. Contrastive learning ablation experiments

With better features extracted from the cross-VAE view and the cross-AAE view (Table 8), we apply a contrastive learning method over these two feature views to get better features in the IP dataset (10% data used in the training process). Results is shown in Table 9.

From Table ??, we can see we get better features with our contrastive methods. In some sense, our method fuses the features from cross-AAE and cross-VAE, which highly improve the performances of the HSI classification task. Higher performance shows our method can extract consistently semantic information for HSI classification downstream tasks.

| Class | Supervised Feature Extraction | | | | Unsupervised Feature Extraction | | | |
|-------|-------------------------------|--------|-------|--------------|---------------------------------|--------|-------------|---------------|
| | SLGDA | 1D-CNN | S-CNN | 3DCAE | AAE | VAE | ContrastNet | Ours model |
| 0 | 98.14 | 97.98 | 99.55 | 100.00 | 99.98 | 99.74 | 99.93 | 100.00 |
| 1 | 99.44 | 99.25 | 99.43 | 99.29 | 100.00 | 99.79 | 99.80 | 100.00 |
| 2 | 99.29 | 94.43 | 98.81 | 97.13 | 100.00 | 100.00 | 99.95 | 100.00 |
| 3 | 99.57 | 99.42 | 97.45 | 97.91 | 99.09 | 99.57 | 98.01 | 100.00 |
| 4 | 98.06 | 96.60 | 97.96 | 98.26 | 99.42 | 99.71 | 99.48 | 99.92 |
| 5 | 99.32 | 99.51 | 99.83 | 99.98 | 99.97 | 99.86 | 99.94 | 99.89 |
| 6 | 99.33 | 99.27 | 99.59 | 99.64 | 99.93 | 99.96 | 99.79 | 100.00 |
| 7 | 89.48 | 86.79 | 94.40 | 91.58 | 91.21 | 86.91 | 99.53 | 99.89 |
| 8 | 99.65 | 99.08 | 98.85 | 99.28 | 99.69 | 99.99 | 99.71 | 100.00 |
| 9 | 97.94 | 93.71 | 97.35 | 96.65 | 98.46 | 96.54 | 99.80 | 99.81 |
| 10 | 99.06 | 94.55 | 97.71 | 97.74 | 99.57 | 100.00 | 99.80 | 99.90 |
| 11 | 100.00 | 99.59 | 98.73 | 98.84 | 100.00 | 99.44 | 99.98 | 100.00 |
| 12 | 97.82 | 97.50 | 96.72 | 99.26 | 99.89 | 97.24 | 98.20 | 96.32 |
| 13 | 90.47 | 94.08 | 95.22 | 97.49 | 99.08 | 96.49 | 98.62 | 100.00 |
| 14 | 69.51 | 66.52 | 95.61 | 87.85 | 93.69 | 87.90 | 99.53 | 99.55 |
| 15 | 99.00 | 97.48 | 99.44 | 98.34 | 99.73 | 99.61 | 99.57 | 100.00 |
| AA(%) | 96.01 | 94.73 | 97.39 | 97.45 | 98.73 | 97.67 | 99.48 | 99.70 |
| OA(%) | 93.31 | 91.30 | 97.92 | 95.81 | 97.10 | 95.23 | 99.60 | 99.82 |

Table 10
Detailed evaluation in Salinas dataset

| Class | Supervised Feature Extraction | | | | Unsupervised Feature Extraction | | | |
|-------|-------------------------------|--------|-------|--------------|---------------------------------|-------|-------------|---------------|
| | SLGDA | 1D-CNN | S-CNN | 3DCAE | AAE | VAE | ContrastNet | Ours model |
| 0 | 94.66 | 90.93 | 95.40 | 95.21 | 95.39 | 81.31 | 99.49 | 100.00 |
| 1 | 97.83 | 96.94 | 97.31 | 96.06 | 98.96 | 97.65 | 99.98 | 100.00 |
| 2 | 77.27 | 69.43 | 81.21 | 91.32 | 97.49 | 91.00 | 99.06 | 99.74 |
| 3 | 93.18 | 90.32 | 95.83 | 98.28 | 96.94 | 94.79 | 97.75 | 99.38 |
| 4 | 98.51 | 99.44 | 99.91 | 95.55 | 99.94 | 99.94 | 99.81 | 100.00 |
| 5 | 90.08 | 73.69 | 95.29 | 95.30 | 99.29 | 99.91 | 99.90 | 100.00 |
| 6 | 85.34 | 83.42 | 87.05 | 95.14 | 100.00 | 99.42 | 99.83 | 99.42 |
| 7 | 90.49 | 83.65 | 87.35 | 91.38 | 97.00 | 94.77 | 98.79 | 99.37 |
| 8 | 99.37 | 98.23 | 95.66 | 99.96 | 96.32 | 88.62 | 94.84 | 95.77 |
| AA(%) | 91.86 | 87.34 | 94.75 | 95.36 | 98.03 | 94.16 | 98.83 | 99.30 |
| OA(%) | 94.15 | 89.99 | 92.78 | 95.39 | 98.14 | 94.53 | 99.46 | 99.78 |

Table 11
Detailed evaluation in University of Pavia dataset

5.3. Detailed contrastive learning experiments of other datasets

Table 10 and Table 11 shows details of our experiments in SA and PU datasets. Because each class's *OA* and *AA* performance are very close, we did not put the details of the experiments in the paper. So we list the detailed performance in the appendix for further analysis. Data in bold are the best performance.

Table 10 shows experiments results in SA dataset. We can see our model also gets state-of-the-art performance with the highest *OA* and highest *AA*. It achieves the best performance for overlapping data (such as classes 10, 11, 12, 13, where other methods may not distinguish well). Our method gets the highest performance from contrastive features. It shows evidence that our cross-representation learning and contrastive strategy can extract better features. For the class 12, performance from

our method decreases a bit. It may be because it is hard to get contrastive features compared with similar classes 10, 11, 13 (all lettuce-romaine).

Table 11 shows experiment results in the PU dataset. We can see our model gets state-of-the-art performance with the highest *OA* and highest *AA*. And in most classes, it achieves the best performance. Our method gains the best performance and outperforms all other existing unsupervised methods. This impressive result shows features from our models have better representation ability. For the class 8, performance from our method decreases a bit. It may come from 'Shadows' data itself. For that, 'Shadows' data has no distinguishable features. It is hard to distinguish 'Shadows' compared with other semantic things, which may confuse contrastive feature extractors. Some dark items may disturb the learning process in our contrastive learning methods. Similarly, *AAE* and *VAE*

also work well in this scenario. Our approach can further enhance the performance of standard auto-encoders and optimize the trade-off between AAE and VAE.

6. Conclusions

In this paper, we proposed a cross-view-prediction style method for HSI feature learning. This style combines the cross-representation learning method and the contrastive learning method. We use this combination to fuse the advantage of the cross-representation learning method (detail texture learning) and contrastive learning method (high-level information learning).

For the cross-representation learning method, we design four typical cross-channel-prediction strategies as augmentation methods to construct different views of original data. Our cross representation learning method naturally suits handling HSI data with highly redundant channels. And this unsupervised cross-channel-prediction task implicitly explores contrastive features in hyperspectral space.

For the contrastive learning method, we propose an interpretable and straightforward contrastive learning method to optimize the features further. More representative and compact features derive from our contrastive learning pipeline, which maximizes mutual information and minimizes conditional entropy across different views.

Based on these two methods, our cross-view-prediction style tends to extract better features with consistent semantics for hyperspectral classification tasks. Our experiments show our proposed method outperforms all existing hyperspectral image classification algorithms.

References

- [1] Martin Arjovsky, Soumith Chintala, and Léon Bottou. Wasserstein generative adversarial networks. In *International conference on machine learning*, pages 214–223. PMLR, 2017.
- [2] Zeyu Cao, Xiaorun Li, Yueming Feng, Shuhan Chen, Chaoqun Xia, and Liaoying Zhao. Contrastnet: Unsupervised feature learning by autoencoder and prototypical contrastive learning for hyperspectral imagery classification. *Neurocomputing*, 460:71–83, 2021.
- [3] Xinlei Chen, Haoqi Fan, Ross Girshick, and Kaiming He. Improved baselines with momentum contrastive learning. *arXiv preprint arXiv:2003.04297*, 2020.
- [4] Xinlei Chen and Kaiming He. Exploring simple siamese representation learning. In *Proceedings of the IEEE/CVF Conference on Computer Vision and Pattern Recognition*, pages 15750–15758, 2021.
- [5] Yushi Chen, Hanlu Jiang, Chunyang Li, Xiuping Jia, and Pedram Ghamisi. Deep feature extraction and classification of hyperspectral images based on convolutional neural networks. *IEEE Transactions on Geoscience and Remote Sensing*, 54(10):6232–6251, 2016.
- [6] Hongmin Gao, Shuo Lin, Yao Yang, Chenming Li, and Mingxiang Yang. Convolution neural network based on two-dimensional spectrum for hyperspectral image classification. *Journal of Sensors*, 2018, 2018.
- [7] Ian Goodfellow, Jean Pouget-Abadie, Mehdi Mirza, Bing Xu, David Warde-Farley, Sherjil Ozair, Aaron Courville, and Yoshua Bengio. Generative adversarial nets. *Advances in neural information processing systems*, 27, 2014.
- [8] Jean-Bastien Grill, Florian Strub, Florent Alché, Corentin Tallec, Pierre H Richemond, Elena Buchatskaya, Carl Doersch, Bernardo Avila Pires, Zhaohan Daniel Guo, Mohammad Gheshlaghi Azar, et al. Bootstrap your own latent: A new approach to self-supervised learning. *arXiv preprint arXiv:2006.07733*, 2020.
- [9] Kaiming He, Haoqi Fan, Yuxin Wu, Saining Xie, and Ross Girshick. Momentum contrast for unsupervised visual representation learning. In *Proceedings of the IEEE/CVF Conference on Computer Vision and Pattern Recognition*, pages 9729–9738, 2020.
- [10] Wei Hu, Yangyu Huang, Li Wei, Fan Zhang, and Hengchao Li. Deep convolutional neural networks for hyperspectral image classification. *Journal of Sensors*, 2015, 2015.
- [11] Xiang Hu, Teng Li, Tong Zhou, Yu Liu, and Yuanxi Peng. Contrastive learning based on transformer for hyperspectral image classification. *Applied Sciences*, 11(18):8670, 2021.
- [12] Xiang Hu, Teng Li, Tong Zhou, and Yuanxi Peng. Deep spatial-spectral subspace clustering for hyperspectral images based on contrastive learning. *Remote Sensing*, 13(21):4418, 2021.
- [13] Diederik P Kingma and Max Welling. Auto-encoding variational bayes. *arXiv preprint arXiv:1312.6114*, 2013.
- [14] Yijie Lin, Yuanbiao Gou, Zitao Liu, Boyun Li, Jiancheng Lv, and Xi Peng. Completer: Incomplete multi-view clustering via contrastive prediction. In *Proceedings of the IEEE/CVF Conference on Computer Vision and Pattern Recognition*, pages 11174–11183, 2021.
- [15] Alireza Makhzani, Jonathon Shlens, Navdeep Jaitly, Ian Goodfellow, and Brendan Frey. Adversarial autoencoders. *arXiv preprint arXiv:1511.05644*, 2015.
- [16] Shaohui Mei, Jingyu Ji, Yunhao Geng, Zhi Zhang, Xu Li, and Qian Du. Unsupervised spatial-spectral feature learning by 3d convolutional autoencoder for hyperspectral classification. *IEEE Transactions on Geoscience and Remote Sensing*, 57(9):6808–6820, 2019.
- [17] Lichao Mou, Pedram Ghamisi, and Xiao Xiang Zhu. Deep recurrent neural networks for hyperspectral image classification. *IEEE Transactions on Geoscience and Remote Sensing*, 55(7):3639–3655, 2017.
- [18] Ingo Steinwart and Andreas Christmann. *Support vector machines*. Springer Science & Business Media, 2008.
- [19] Chao Tao, Hongbo Pan, Yansheng Li, and Zhengrou Zou. Unsupervised spectral-spatial feature learning with stacked sparse autoencoder for hyperspectral imagery classification. *IEEE*

- Geoscience and remote sensing letters*, 12(12):2438–2442, 2015.
- [20] Laurens Van der Maaten and Geoffrey Hinton. Visualizing data using t-sne. *Journal of machine learning research*, 9(11), 2008.
- [21] Alberto Villa, Jon Atli Benediktsson, Jocelyn Chanussot, and Christian Jutten. Hyperspectral image classification with independent component discriminant analysis. *IEEE transactions on Geoscience and remote sensing*, 49(12):4865–4876, 2011.
- [22] Di Wang, Bo Du, and Liangpei Zhang. Fully contextual network for hyperspectral scene parsing. *IEEE Transactions on Geoscience and Remote Sensing*, 2021.
- [23] Di Wang, Bo Du, Liangpei Zhang, and Yonghao Xu. Adaptive spectral–spatial multiscale contextual feature extraction for hyperspectral image classification. *IEEE Transactions on Geoscience and Remote Sensing*, 59(3):2461–2477, 2020.
- [24] Xue Wang, Kun Tan, Qian Du, Yu Chen, and Peijun Du. Cva²: A conditional variational autoencoder with an adversarial training process for hyperspectral imagery classification. *IEEE Transactions on Geoscience and Remote Sensing*, 58(8):5676–5692, 2020.
- [25] Svante Wold, Kim Esbensen, and Paul Geladi. Principal component analysis. *Chemometrics and intelligent laboratory systems*, 2(1-3):37–52, 1987.
- [26] Zhenda Xie, Yutong Lin, Zheng Zhang, Yue Cao, Stephen Lin, and Han Hu. Propagate yourself: Exploring pixel-level consistency for unsupervised visual representation learning. In *Proceedings of the IEEE/CVF Conference on Computer Vision and Pattern Recognition*, pages 16684–16693, 2021.
- [27] Wenbo Yu, Miao Zhang, and Yi Shen. Spatial revising variational autoencoder-based feature extraction method for hyperspectral images. *IEEE Transactions on Geoscience and Remote Sensing*, 59(2):1410–1423, 2021.
- [28] Richard Zhang, Phillip Isola, and Alexei A Efros. Split-brain autoencoders: Unsupervised learning by cross-channel prediction. In *Proceedings of the IEEE Conference on Computer Vision and Pattern Recognition*, pages 1058–1067, 2017.
- [29] Zilong Zhong, Jonathan Li, Zhiming Luo, and Michael Chapman. Spectral–spatial residual network for hyperspectral image classification: A 3-d deep learning framework. *IEEE Transactions on Geoscience and Remote Sensing*, 56(2):847–858, 2017.